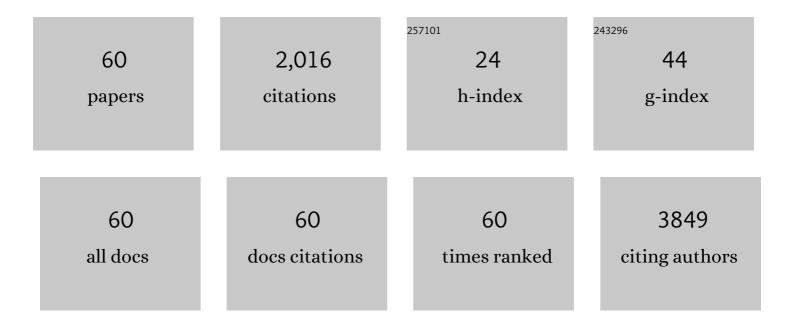
## Alexander S Walton

List of Publications by Year in descending order

Source: https://exaly.com/author-pdf/3931539/publications.pdf Version: 2024-02-01



#	Article	IF	CITATIONS
1	Corrosion inhibition in acidic environments: key interfacial insights with photoelectron spectroscopy. Faraday Discussions, 2022, 236, 374-388.	1.6	6
2	Universal shape of graphene nanobubbles on metallic substrate. Physical Chemistry Chemical Physics, 2022, 24, 6935-6940.	1.3	9
3	Direct <i>in situ</i> spectroscopic evidence of the crucial role played by surface oxygen vacancies in the O <sub>2</sub> -sensing mechanism of SnO <sub>2</sub> . Chemical Science, 2022, 13, 6089-6097.	3.7	7
4	Nanocubes of Mo <sub>6</sub> S <sub>8</sub> Chevrel phase as active electrode material for aqueous lithium-ion batteries. Nanoscale, 2022, 14, 10125-10135.	2.8	9
5	A combined laboratory and synchrotron in-situ photoemission study of the rutile TiO <sub>2</sub> (110)/water interface. Journal Physics D: Applied Physics, 2021, 54, 194001.	1.3	6
6	Oleylamine Aging of PtNi Nanoparticles Giving Enhanced Functionality for the Oxygen Reduction Reaction. Nano Letters, 2021, 21, 3989-3996.	4.5	37
7	Intrinsic effects of thickness, surface chemistry and electroactive area on nanostructured MoS2 electrodes with superior stability for hydrogen evolution. Electrochimica Acta, 2021, 382, 138257.	2.6	9
8	Role of Alkali Cations in Stabilizing Mixed-Cation Perovskites to Thermal Stress and Moisture Conditions. ACS Applied Materials & Interfaces, 2021, 13, 43573-43586.	4.0	16
9	Manipulation of Molecular Vibrations on Condensing Er3+ State Densities for 1.5 μm Application. Journal of Physical Chemistry Letters, 2021, 12, 9620-9625.	2.1	1
10	High-Performance Nanostructured MoS <sub>2</sub> Electrodes with Spontaneous Ultralow Gold Loading for Hydrogen Evolution. Journal of Physical Chemistry C, 2021, 125, 20940-20951.	1.5	9
11	Nanoscale Chevrel-Phase Mo <sub>6</sub> S <sub>8</sub> Prepared by a Molecular Precursor Approach for Highly Efficient Electrocatalysis of the Hydrogen Evolution Reaction in Acidic Media. ACS Applied Energy Materials, 2021, 4, 13015-13026.	2.5	12
12	Formation of a U(VI)–Persulfide Complex during Environmentally Relevant Sulfidation of Iron (Oxyhydr)oxides. Environmental Science & Technology, 2020, 54, 129-136.	4.6	17
13	An Exemplar Imidazoline Surfactant for Corrosion Inhibitor Studies: Synthesis, Characterization, and Physicochemical Properties. Journal of Surfactants and Detergents, 2020, 23, 225-234.	1.0	15
14	PtNi bimetallic structure supported on UiO-67 metal-organic framework (MOF) during CO oxidation. Journal of Catalysis, 2020, 391, 522-529.	3.1	7
15	Photo-Seebeck study of amorphous germanium–tellurium-oxide films. Journal of Materials Science: Materials in Electronics, 2020, 31, 22000-22011.	1.1	1
16	Intercalation, decomposition, entrapment – a new route to graphene nanobubbles. Physical Chemistry Chemical Physics, 2020, 22, 7606-7615.	1.3	10
17	Core level photoemission line shape selection: Atomic adsorbates on iron. Surface and Interface Analysis, 2020, 52, 507-512.	0.8	6
18	Hydrogenation of benzoic acid to benzyl alcohol over Pt/SnO2. Applied Catalysis A: General, 2020, 593, 117420	2.2	15

ALEXANDER S WALTON

#	Article	IF	CITATIONS
19	Use of titanocalix[4]arenes in the ring opening polymerization of cyclic esters. Catalysis Science and Technology, 2020, 10, 1619-1639.	2.1	25
20	Room-Temperature Production of Nanocrystalline Molybdenum Disulfide (MoS <sub>2</sub> ) at the Liquidâ^'Liquid Interface. Chemistry of Materials, 2019, 31, 5384-5391.	3.2	16
21	Air-Stable Methylammonium Lead Iodide Perovskite Thin Films Fabricated via Aerosol-Assisted Chemical Vapor Deposition from a Pseudohalide Pb(SCN) <sub>2</sub> Precursor. ACS Applied Energy Materials, 2019, 2, 6012-6022.	2.5	13
22	Modulating Crystallization in Semitransparent Perovskite Films Using Submicrometer Spongelike Polymer Colloid Particles to Improve Solar Cell Performance. ACS Applied Energy Materials, 2019, 2, 6624-6633.	2.5	14
23	Adsorption site, orientation and alignment of NO adsorbed on Au(100) using 3D-velocity map imaging, X-ray photoelectron spectroscopy and density functional theory. Physical Chemistry Chemical Physics, 2019, 21, 10939-10946.	1.3	11
24	Structure and Stability of Au-Supported Layered Cobalt Oxide Nanoislands in Ambient Conditions. Journal of Physical Chemistry C, 2019, 123, 9176-9182.	1.5	14
25	Optical Study of p-Doping in GaAs Nanowires for Low-Threshold and High-Yield Lasing. Nano Letters, 2019, 19, 362-368.	4.5	24
26	Phase Transitions of Cobalt Oxide Bilayers on Au(111) and Pt(111): The Role of Edge Sites and Substrate Interactions. Journal of Physical Chemistry B, 2018, 122, 561-571.	1.2	26
27	Water-induced reordering in ultrathin ionic liquid films. Journal of Physics Condensed Matter, 2018, 30, 334003.	0.7	8
28	Decoupling Structure and Composition of CH <sub>3</sub> NH <sub>3</sub> Pbl <sub>3–<i>x</i></sub> Br <sub><i>x</i></sub> Films Prepared by Combined One-Step and Two-Step Deposition. ACS Applied Energy Materials, 2018, 1, 5567-5578.	2.5	9
29	Understanding the CO Oxidation on Pt Nanoparticles Supported on MOFs by <i>Operando</i> XPS. ChemCatChem, 2018, 10, 4238-4242.	1.8	35
30	Ambient-air-stable inorganic Cs <sub>2</sub> SnI <sub>6</sub> double perovskite thin films <i>via</i> aerosol-assisted chemical vapour deposition. Journal of Materials Chemistry A, 2018, 6, 11205-11214.	5.2	85
31	Edge reactivity and water-assisted dissociation on cobalt oxide nanoislands. Nature Communications, 2017, 8, 14169.	5.8	117
32	In situ investigation of degradation at organometal halide perovskite surfaces by X-ray photoelectron spectroscopy at realistic water vapour pressure. Chemical Communications, 2017, 53, 5231-5234.	2.2	78
33	Gold-supported two-dimensional cobalt oxyhydroxide (CoOOH) and multilayer cobalt oxide islands. Physical Chemistry Chemical Physics, 2017, 19, 2425-2433.	1.3	38
34	The offset droplet: a new methodology for studying the solid/water interface using x-ray photoelectron spectroscopy. Journal of Physics Condensed Matter, 2017, 29, 454001.	0.7	17
35	Comparative Analysis of Cobalt Oxide Nanoisland Stability and Edge Structures on Three Related Noble Metal Surfaces: Au(111), Pt(111) and Ag(111). Topics in Catalysis, 2017, 60, 503-512.	1.3	29
36	Nanostructured Aptamer-Functionalized Black Phosphorus Sensing Platform for Label-Free Detection of Myoglobin, a Cardiovascular Disease Biomarker. ACS Applied Materials & Interfaces, 2016, 8, 22860-22868.	4.0	208

3

ALEXANDER S WALTON

#	Article	IF	CITATIONS
37	Investigation of the Differential Capacitance of Highly Ordered Pyrolytic Graphite as a Model Material of Graphene. Langmuir, 2016, 32, 11448-11455.	1.6	43
38	Controlling the Electrical Transport Properties of Nanocontacts to Nanowires. Nano Letters, 2015, 15, 4248-4254.	4.5	34
39	Interface Controlled Oxidation States in Layered Cobalt Oxide Nanoislands on Gold. ACS Nano, 2015, 9, 2445-2453.	7.3	78
40	Vanadyl calix[6]arene complexes: synthesis, structural studies and ethylene homo-(co-)polymerization capability. Dalton Transactions, 2015, 44, 12292-12303.	1.6	27
41	<i>In Situ</i> Detection of Active Edge Sites in Single-Layer MoS <sub>2</sub> Catalysts. ACS Nano, 2015, 9, 9322-9330.	7.3	144
42	ZnO nanowires with Au contacts characterised in the as-grown real device configuration using a local multi-probe method. Nanotechnology, 2014, 25, 425706.	1.3	11
43	Patchiness of ion-exchanged mica revealed by DNA binding dynamics at short length scales. Nanotechnology, 2014, 25, 025704.	1.3	10
44	Examining the crystal growth that influences the electronic device output from vertical arrays of ZnO nanowires. Materials Research Society Symposia Proceedings, 2014, 1659, 101-106.	0.1	0
45	Reversible metallisation of soft UV patterned substrates. Journal of Materials Chemistry C, 2014, 2, 5916-5923.	2.7	4
46	Structure and Electronic Properties of <i>In Situ</i> Synthesized Single-Layer MoS <sub>2</sub> on a Gold Surface. ACS Nano, 2014, 8, 6788-6796.	7.3	136
47	MoS2 nanoparticle morphologies in hydrodesulfurization catalysis studied by scanning tunneling microscopy. Journal of Catalysis, 2013, 308, 306-318.	3.1	101
48	Vanadium(iii) phenoxyimine complexes for ethylene or ε-caprolactone polymerization: mononuclear versus binuclear pre-catalysts. Catalysis Science and Technology, 2013, 3, 152-160.	2.1	36
49	Factors that determine and limit the resistivity of high-quality individual ZnO nanowires. Nanotechnology, 2013, 24, 435706.	1.3	39
50	Highly Active, Thermally Stable, Ethylene-Polymerisation Pre-Catalysts Based on Niobium/TantalumImine Systems. Chemistry - A European Journal, 2013, 19, 8884-8899.	1.7	22
51	An investigation of the growth of bismuth whiskers and nanowires during physical vapour deposition. Journal Physics D: Applied Physics, 2012, 45, 435304.	1.3	22
52	Origin of significant visible-light absorption properties of Mn-doped TiO2 thin films. Acta Materialia, 2012, 60, 1974-1985.	3.8	56
53	Low-Temperature Preparation of Single Crystal Titanium Carbide Nanofibers in Molten Salts. Crystal Growth and Design, 2011, 11, 3122-3129.	1.4	30
54	Evaporation and decomposition of acrylic acid grafted luminescent silicon quantum dots in ultrahigh vacuum. Journal of Physics: Conference Series, 2011, 286, 012039.	0.3	0

ALEXANDER S WALTON

#	Article	IF	CITATIONS
55	Zirconium as a Boron Sink in Crystalline CoFeB/MgO/CoFeB Magnetic Tunnel Junctions. Applied Physics Express, 2011, 4, 013002.	1.1	19
56	Synthesis of High‧urfaceâ€Area Platinum Nanotubes Using a Viral Template. Advanced Functional Materials, 2010, 20, 1295-1300.	7.8	118
57	Photoelectric Properties of Electrodeposited Copper(I) Oxide Nanowires. Journal of the Electrochemical Society, 2009, 156, K191.	1.3	13
58	Four-probe electrical characterization of Pt-coated TMV-based nanostructures. Nanotechnology, 2008, 19, 165704.	1.3	32
59	Magnetic field enhanced nano-tip fabrication for four-probe STM studies. Nanotechnology, 2008, 19, 085201.	1.3	11
60	Four-probe electrical transport measurements on individual metallic nanowires. Nanotechnology, 2007, 18, 065204.	1.3	71